

# VC dimension of Graph Neural Networks with Pfaffian activation functions

Giuseppe Alessio D’Inverno, Monica Bianchini, Franco Scarselli

Department of Information Engineering and Mathematics, University of Siena, Via Roma 56, Siena, 53100, (SI), Italy

January 24, 2024

## Abstract

Graph Neural Networks (GNNs) have emerged in recent years as a powerful tool to learn tasks across a wide range of graph domains in a data-driven fashion; based on a message passing mechanism, GNNs have gained increasing popularity due to their intuitive formulation, closely linked with the Weisfeiler-Lehman (WL) test for graph isomorphism, to which they have proven equivalent [1, 2]. From a theoretical point of view, GNNs have been shown to be universal approximators, and their generalization capability (namely, bounds on the Vapnik Chervonekis (VC) dimension [3]) has recently been investigated for GNNs with piecewise polynomial activation functions [4]. The aim of our work is to extend this analysis on the VC dimension of GNNs to other commonly used activation functions, such as sigmoid and hyperbolic tangent, using the framework of Pfaffian function theory. Bounds are provided with respect to architecture parameters (depth, number of neurons, input size) as well as with respect to the number of colors resulting from the 1-WL test applied on the graph domain. The theoretical analysis is supported by a preliminary experimental study.

## 1 Introduction

Since Deep Learning has become involved more and more in real-life applications [5, 6, 7, 8], the urge of investigating its theoretical properties has become more prominent. Neural networks have been then progressively studied analyzing for instance their expressive power in terms of approximating classes of functions [9, 10, 11, 12] or showing their limitations in neurocognitive

tasks imitation [13, 14, 15]. The *generalization capability* of a learning model, intended as the capacity of correctly performing a specific task on unseen data, has always been a core aspect to evaluate the effectiveness of proposed architectures [16, 17]. Several metrics and/or methods have been proposed over the years to evaluate such capability [18, 19]. Among them we find the *Vapnik Chervonenkis (VC) dimension* [20], which is a metric that measures the capacity of a learning model to *shatter* a set of data points, given any binary labelling. Intuitively, greater the VC dimension of the learning model, the more it will fit the data on which it has been trained. On the other hand, as it has been shown in [21], large VC dimensions leads to a poor generalization, namely a large difference is expected between the error on train set and the error on test set. It is then important to be able to evaluate the VC dimension of a model, especially with respect to its hyperparameters, in order to design an efficient architecture capable of generalizing outside the training data.

Graph Neural Networks (GNNs) [22, 23] are machine learning architectures capable of processing graphs that represent patterns (or part of patterns along) their relationships. GNNs are among the most used deep learning models nowadays, given the impressive performance they have shown in tasks related to structured data [24]. A great effort has been dedicated to assess their expressive power, mainly related to the study of the so-called Weisfeiler-Lehman (WL) test [25] and its variants [1, 26, 27]. Indeed, the standard WL algorithm, which operates by iteratively assigning colors to the nodes of the input graph and is a method to test whether two graphs are isomorphic or not, has been proved to be equivalent to GNNs in terms of the capability of distinguishing graphs [2]. On the other hand, very little is known about their generalization capabilities. In [3], bounds for the VC dimension have been provided for the original GNN model, namely the first model being introduced. Very recently [4] bounds have been found also for a large class of modern GNNs with piecewise polynomial activation functions. Nevertheless, message passing GNNs with other common activation functions such as hyperbolic tangent, sigmoid and arctangent still lack of a characterization in terms of VC dimension.

This work aims to close this gap, providing new bounds for modern message passing GNNs with Pfaffian activation functions. The *Pfaffian functions* are a large class of differentiable maps, which includes the above mentioned common activation functions, i.e, `tanh`, `logsig`, `atan`, and, more generally, most of the function used in Engineering having continuous derivatives up to any order. We list our contributions as follow:

- We provide upper bounds for message passing GNNs with Pfaffian activation functions with respect to the main hyperparameters, such as the feature dimension, the hidden feature size, the number of message passing layers implemented and the total number of nodes in the training domain. To prove these results we exploit theoretical results in literature that link the theory of Pfaffian function and the characterization of the VC dimension of the model via topological analysis.
- We also study the trend of the VC dimension w.r.t. the total number of the different colors in the dataset obtained by running the WL test. The theoretical result suggests that the number of colors have an important effect on GNN generalization capability. On one hand, a large total number of colors in training set improves generalization, since it increases the examples available for learning; on the other hand, a larger number of colors in each graph raises the VC dimension and therefore it increases the empirical risk value.
- Our theoretical findings are experimentally assessed by a preliminary experimental study; in specific, we evaluate the gap between the predictive performance on the training data and the one on unseen data.

The manuscript is organized as follow. In Section 2 we offer an overview of the related work on the topic. In Section 3 we introduce the main concepts and the notation used throughout the manuscript. In Section 4 we state and discuss our main theoretical results. In Section 5 we report the experimental validation of the main results. Finally, in Section 6 we summarize the content of the manuscript, providing a brief discussion about open problems and future directions.

## 2 Related Work

**Generalization bounds for GNNs** Several approaches have been exploited in order to give some insights about the generalization abilities of GNNs. In [28] the generalization ability of GNNs is studied by providing new bounds on the *Rademacher complexity* in binary classification tasks; the study is carried out by focusing on the computation trees of the nodes, which are tightly linked to the 1-order WL test [29] [30]. Similarly, in [31] the authors derive generalization bounds for GCNs based on Transductive Rademacher Complexity, which differs from the standard Rademacher Complexity by taking into account unobserved instances. The authors of [32]

prove that the stability, and consequently the generalization capabilities of Graph Convolutional Networks (GCNs), depend on the largest eigenvalue of the convolutional filter; therefore, to ensure a better generalization capability, the eigenvalue should be independent of the graph size. Under the lens of the PAC-learnability framework, the generalization bounds of [28] have been improved in [33], showing a tighter dependency on the maximum node degree and the spectral norm for the weights. This result aligns with the findings in [32]. In [34], the authors provide sharper bounds on the GNNs stability to noise by investigating the correlation between attention and generalization in GNNs: specifically GCNs and Graph Isomorphism Networks (GINs) are considered. The results show a link between the trace of the Hessians of the weight matrices and the stability of GNNs. A correlation between attention and generalization in GCNs and GINs is empirically investigated in [35].

**VC dimension** Since it was first introduced in [20], the VC dimension has become a widespread metric to assess the generalization capabilities of neural networks. In [36] the VC dimension is proven to be tightly related to how the test error is distant from the training error, in probability. Bounds on the VC dimension have been provided for many baseline architectures, such as Multi Layer Perceptrons (MLPs) [37] [38], Recurrent Neural Networks (RNNs) [39] and Recursive Neural Networks [3]. In [3], bounds on the VC dimension of the earliest GNN model with Pfaffian activation function are provided as well. Our work extends those results to generic GNNs of the form (2). The authors of [31] provide bounds on the VC dimension of GCNs for linear and ReLU activation functions.

Our results are particularly related to the work in [4] where bounds for the VC dimension of modern GNNs are studied, when the activation function is a piecewise linear polynomial function. Bounds are derived also in terms of the number of colors computed by the 1-order WL test on the graph domain.

Nevertheless, aside from [3], all the aforementioned works focus solely on specific GNN models with piecewise polynomials activation functions, leaving out all GNN models with other common activation functions as arctangent, hyperbolic tangent or sigmoid.

**Pfaffian functions** Pfaffian functions have been first introduced in [40] to extend Bezout’s classic theorem, which states that the number of complex solutions of a set of polynomial equations can be estimated based on their degree. The theory of Pfaffian functions has been exploited initially in [41] to characterize the bounds of the VC dimension of neural networks. Similarly, in

[3] the same approach is used to provide the aforementioned bounds. Pfaffian functions have been revealed useful also to give insights on the topological complexity of neural networks and on the role of their depth [42].

### 3 Notation and basic concepts

In this section we introduce the notation used throughout the sections and the main basic concepts necessary to understand the content of this work.

**Graphs** An *unattributed graph*  $G$  can be defined as a couple  $(V, E)$ , where  $V$  is the (finite) set of *nodes* and  $E \subseteq V \times V$  is the set of *edges* between nodes. A graph can be defined by its *adjacency matrix*  $A$ , where  $A_{ij} = 1$  if  $e_{ij} = (i, j) \in E$ , otherwise  $A_{ij} = 0$ . The *neighborhood* of a node  $v$  is defined as  $ne(v) = \{u \in V | (u, v) \in E, (v, u) \in E\}$ . A graph  $G$  is said to be *undirected* if it is assumed that  $(v, u) = (u, v)$  (and therefore its adjacency matrix is symmetric), *directed* otherwise. A graph can be said to be *node-attributed* if there exists a map  $\alpha : V \rightarrow \mathbb{R}^q$  that assigns to every  $v \in V$  a *node attribute*  $\alpha(v) \in \mathbb{R}^q$ .

**The 1-WL test** The *1st order Weisfeiler Lehman test* (briefly, the *1-WL test*) is a test for graph isomorphism, based on the so-called *color refinement* procedure. Given two graphs  $G_1 = (V_1, E_1)$  and  $G_2 = (V_2, E_2)$  in a finite graph domain  $\mathcal{G}$ , we perform the following steps.

- At initialization, we assign a color  $c^{(0)}(v)$  to each node  $v \in V_1 \cup V_2$ . Formally, in the case of attributed graphs, we can define the color initialisation

$$c^{(0)}(v) = \text{HASH}_0(\ell_v),$$

where  $\text{HASH}_0 : \mathbb{R}^q \rightarrow \Sigma$  is a function that codes bijectively node attributes to colors. In case of unattributed graphs, the initialisation is uniform, and each node  $v$  gets the same color  $c^{(0)}(v)$ .

- For  $t > 0$ , we update the color of each node in parallel on each graph by the following updating scheme

$$c_v^{(t)} = \text{HASH}(c_v^{(t-1)}, \{\{c_u^{(t-1)} | u \in ne[v]\}\}) \quad \forall v \in V_1 \cup V_2, \quad (1)$$

where  $\text{HASH} : \Sigma \times \Sigma^* \rightarrow \Sigma$  is a function mapping bijectively a couple (color, colors multiset) to a single color.

To test whether the two graphs  $G_1, G_2$  are isomorphic or not, the set of colors of  $G_1, G_2$  are compared step by step; if there exist an iteration  $t$  such that the colors are different, namely  $c_{G_1}^{(t)} := \{\{c^{(t)}(v) \mid v \in V_1\}\}$  is different from  $c_{G_2}^{(t)}$ , the graphs are determined as non-isomorphic. When no difference is detected, the procedure halts as soon the node partition defined by the colors becomes stable. It has been proven [43] that  $|V| - 1$  iterations are sufficient, and sometimes necessary, to complete the procedure. On the other hand, the color refinement procedure can be used also to test whether two nodes are isomorphic or not. Intuitively, two nodes are isomorphic if their neighborhoods (of any order) are equal; such an isomorphism can be tested by comparing the node colors at any step of 1-WL. In [29] it has been proven that for node isomorphism up to  $2 \max(|V_1|, |V_2|) - 1$  refinements steps may be required.

We would like to bring to mind two important findings that prove the equivalence between GNNs and 1-WL test in terms of their expressive power. The first result was established in [2], which characterizes the equivalence of GNNs and 1-WL test on a graph-level task. This equivalence is based on GNNs with generic message passing layers that satisfy certain conditions. Another characterization is due to [1] and states the equivalence on a node coloring level, referring to the particular model defined by Eq. (3).

**Graph Neural Networks (GNNs)** Graph Neural Networks are a class of machine learning models suited to process structured data in form of graphs. At a high level, we can formalize a GNN as a function  $g : \mathcal{G} \rightarrow \mathbb{R}^r$ , where  $\mathcal{G}$  is a set of node-attributed graphs and  $r$  is the dimension of the output, which depends on the type of task at hand. Intuitively, a GNN learns how to represent the nodes of a graph by vectorial representations, called *hidden features*, giving an encoding of the information stored in the graph. The computation paradigm underlying GNNs relies on stacking layers of the form

$$h_v^{(t+1)} = \text{COMBINE}^{(t+1)}(h_v^{(t)}, \text{AGGREGATE}^{(t+1)}(\{\{h_u^{(t)} \mid u \in \text{ne}(v)\}\})), \quad (2)$$

for all  $v \in V$  and  $t = 1, \dots, T$ , where  $h_v^{(t)}$  is the hidden feature of node  $v$  at time  $t$ ,  $T$  is the number of layers of the GNN and  $\{\cdot\}$  denotes a multiset. Here  $\{\text{COMBINE}^{(t)}\}_{t=1, \dots, T}$  and  $\{\text{AGGREGATE}^{(t)}\}_{t=1, \dots, T}$  are families of functions that can be defined by learning from examples. Popular GNN models like GraphSAGE [44], GCN [45], Graph Isomorphism Networks [2] are based on this updating scheme. The output  $o$  is produced by a **READOUT** function, which, in graph focused tasks, takes in input the features of all the nodes, i.e.

$o_V = \text{READOUT}(\{\{h_u^{(T)} | u \in V\}\})$ , and, in node focused tasks, takes in input the feature of a node, i.e.,  $o = \text{READOUT}(h_u^{(T)})$ .

We will assume in the following, for ease of computation, that the number of parameters of  $\text{COMBINE}^{(t)}$  is the same for every  $t = 1, \dots, T$ , and we denote it as  $p_{\text{comb}}$ . The same holds for  $\text{AGGREGATE}^{(t)}$  and  $\text{READOUT}$  with the number of parameters denoted respectively as  $p_{\text{agg}}$  and  $p_{\text{read}}$ . Thus, the total number of parameters in a GNN defined as in Eq. (2) is  $\bar{p} = L(p_{\text{comb}} + p_{\text{agg}}) + p_{\text{read}}$ .

For our analysis, following [1], we also consider a simpler computation framework, which has been proven to match the expressive power of the Weisfeiler-Lehman test [1], and is general enough to be similar to many GNN models.

In such a framework, the hidden feature  $h_v^{(t+1)} \in \mathbb{R}^h$  of a node  $v$  at the message passing iteration  $t + 1$  is defined as

$$h_v^{(t+1)} = \sigma(\mathbf{W}_{\text{comb}}^{(t+1)} h_v^{(t)} + \mathbf{W}_{\text{agg}}^{(t+1)} h_{\text{ne}(v)}^{(t)} + \mathbf{b}^{(t+1)}), \quad (3)$$

where  $h_{\text{ne}(v)}^{(t)} = \text{POOL}(\{\{h_u^{(t)} | u \in \text{ne}(v)\}\})$ ,  $\sigma : \mathbb{R}^h \rightarrow \mathbb{R}^h$  is an element-wise activation function and  $\text{POOL}$  is the aggregating operator on the neighbor node's features,

$$\text{POOL}(\{\{h_u^{(t)} | u \in \text{ne}(v)\}\}) = \sum_{u \in \text{ne}(v)} h_u^{(t)}. \quad (4)$$

With respect to equation (2), we have that  $\text{AGGREGATE}^{(t)}(\cdot) = \text{POOL}(\cdot) \forall t = 1, \dots, T$ , while  $\text{COMBINE}^{(t+1)}(h_v, h_{\text{ne}(v)}) = \sigma(W_{\text{comb}}^{(t+1)} h_v + W_{\text{agg}}^{(t+1)} h_{\text{ne}(v)} + b^{(t+1)})$ .

In this case, the  $\text{READOUT}$  for graph classification tasks has been defined as

$$\text{READOUT}(\{h_v^{(L)} | v \in V\}) := f\left(\sum_{v \in V} h_v^{(L)} \mathbf{w} + b\right) \quad (5)$$

For each node, the initial hidden state is initialized as  $h_v^{(0)} = \alpha_v \in \mathbb{R}^k$ . The learnable parameters of the GNN can be summarized as

$$\Theta := (W_{\text{comb}}^{(0)}, W_{\text{agg}}^{(0)}, b^{(0)}, W_{\text{comb}}^{(1)}, W_{\text{agg}}^{(1)}, b^{(1)}, \dots, W_{\text{comb}}^{(L)}, W_{\text{agg}}^{(L)}, b^{(L)}),$$

with  $W_{\text{comb}}^{(0)}, W_{\text{agg}}^{(0)} \in \mathbb{R}^{k \times h}$ ,  $W_{\text{comb}}^{(t)}, W_{\text{agg}}^{(t)} \in \mathbb{R}^{h \times h}$ , for  $t = 1, \dots, T$ , and  $b^{(t)} \in \mathbb{R}^h$ , for  $t = 0, \dots, T$ .

**VC dimension** The VC dimension is a measure of complexity of a hypothesis set, which can be used to bound the empirical error of machine learning models. Formally, a binary classifier  $\mathcal{L}$  with parameters  $\theta$  is said to *shatter* a set of patterns  $\{x_1, \dots, x_n\}$  if, for any binary labeling of the examples  $\{y_i\}_{i=1, \dots, n}$ ,  $y_i \in \{0, 1\}$ , there exists  $\theta$  s.t. the model  $\mathcal{L}$  correctly classifies all the patterns, i.e.  $\sum_{i=1}^n |\mathcal{L}(\theta, x_i) - y_i| = 0$ . The *VC dimension* of the model  $\mathcal{L}$  is the dimension of the largest set that  $\mathcal{L}$  can shatter.

The VC dimension has been linked with the generalization capability of machine learning models. Actually, given a training set and a test set for the classifier  $\mathcal{L}$ , whose patterns are i.i.d. samples extracted from the same distribution, the VC dimension allows to compute a bound the difference between training and test error. Formally, it has been proved [46] that, for any  $\eta > 0$ ,

$$\Pr(\text{test error} \leq \text{training error} + \sqrt{\frac{1}{N} [\text{VCdim}(\log(\frac{2N}{\text{VCdim}}) + 1) - \log(\frac{\eta}{4})]) = 1 - \eta \quad (6)$$

holds, where  $N$  is the size of the training dataset and  $\text{VCdim}$  the VC dimension of  $L$ .

**Pfaffian Functions** Formally, a Pfaffian chain of order  $\ell \geq 0$  and degree  $\alpha \geq 1$  in an open domain  $U \subseteq \mathbb{R}^n$  is a sequence of analytic functions  $f_1, f_2, \dots, f_\ell$  in  $U$  satisfying the differential equations

$$df_j(\mathbf{x}) = \sum_{1 \leq i \leq n} g_{ij}(\mathbf{x}, f_1(\mathbf{x}), \dots, f_j(\mathbf{x})) dx_i$$

for  $1 \leq j \leq \ell$ . Here, the  $g_{ij}(\mathbf{x}, y_1, \dots, y_j)$  are polynomials in  $\mathbf{x} \in U$  and  $y_1, \dots, y_j \in \mathbb{R}$  of degrees not exceeding  $\alpha$ . A function  $f(\mathbf{x}) = P(\mathbf{x}, f_1(\mathbf{x}), \dots, f_\ell(\mathbf{x}))$ , where  $P(\mathbf{x}, y_1, \dots, y_\ell)$  is a polynomial of degree not exceeding  $\beta$ , is called a *Pfaffian function of format*  $\text{format}(f) = (\alpha, \beta, \ell)$ .

The Pfaffian maps are a large class of functions that include most of the functions with continuous derivatives used in practical applications [40]. For what it is related to this manuscript, we mention that the arctangent `atan`, the logistic sigmoid `logsig` and the hyperbolic tangent `tanh` are Pfaffian functions, with  $\text{format}(\text{atan}) = (3, 1, 2)$ ,  $\text{format}(\text{logsig}) = (2, 1, 1)$ , and  $\text{format}(\text{tanh}) = (2, 1, 1)$ , respectively.



## 4 Results

In this section we report the main results on the VC dimension of GNNs with Pfaffian activation functions. The proofs can be found in Appendix A.

### 4.1 Main bounds

Our main result provides a bound on VC dimension of general GNNs with Pfaffian activation function and on GNNs with logistic sigmoid activation function w.r.t. the total number  $\bar{p}$  of parameters, the number of computation units  $H$ , the number of layers  $L$ , the feature dimension  $d$ , the maximum number  $N$  of nodes in a graph, the attribute dimension  $q$ . Here, we assume that GNN computation units include the neurons computing the hidden features and the outputs. Thus, there is a computation unit for each component of a feature, each layer, each node of the input graph and a further computation unit for the READOUT.

**Theorem 1.** Let us consider the GNN model described by Eq. (2). If  $\text{COMBINE}^{(t)}$ ,  $\text{AGGREGATE}^{(t)}$  and  $\text{READOUT}$  be Pfaffian functions with format, respectively,  $(\alpha_{\text{comb}}, \beta_{\text{comb}}, \ell_{\text{comb}})$ ,  $(\alpha_{\text{agg}}, \beta_{\text{agg}}, \ell_{\text{agg}})$ ,  $(\alpha_{\text{read}}, \beta_{\text{read}}, \ell_{\text{read}})$  then the VC dimension satisfies

$$\text{VCdim}(\text{GNN}) \leq 2 \log B + \bar{p}(16 + 2 \log \bar{s})$$

where  $B \leq 2^{\frac{\bar{\ell}(\bar{\ell}-1)}{2}+1}(\bar{\alpha} + 2\bar{\beta} - 1)^{\bar{p}-1}((2\bar{p} - 1)(\bar{\alpha} + \bar{\beta}) - 2\bar{p} + 2)^{\bar{\ell}}$ ,  $\bar{\alpha} = \max\{\alpha_{\text{agg}}, \alpha_{\text{comb}}, \alpha_{\text{read}}\}$ ,  $\bar{\beta} = \max\{\beta_{\text{comb}}, \beta_{\text{read}}\}$ ,  $H = LNd(\ell_{\text{comb}} + \ell_{\text{agg}}) + \ell_{\text{read}}$ ,  $\bar{p} = L(p_{\text{comb}} + p_{\text{agg}}) + p_{\text{read}}$ ,  $\bar{\ell} = \bar{p}H$ , and  $\bar{s} = LNd + Nq + 1$  hold.

By substituting in the variables, we obtain

$$\begin{aligned} \text{VCdim}(\text{GNN}) &\leq (L(p_{\text{comb}} + p_{\text{agg}}) + p_{\text{read}})^2 (LNd(\ell_{\text{comb}} + \ell_{\text{agg}}) + \ell_{\text{read}})^2 \\ &\quad + 2(L(p_{\text{comb}} + p_{\text{agg}}) + p_{\text{read}}) \log(3\gamma) \\ &\quad + 2(L(p_{\text{comb}} + p_{\text{agg}}) + p_{\text{read}}) \log((4\gamma - 2)(L(p_{\text{comb}} + p_{\text{agg}}) + p_{\text{read}} + 2 - 2\gamma)) \\ &\quad + (L(p_{\text{comb}} + p_{\text{agg}}) + p_{\text{read}})(16 + 2 \log(LNd + Nq + 1)), \end{aligned}$$

By inspecting the bound, we observe that the dominant term is  $\bar{p}^2 H^2 = \bar{p}^2 (LNd(\ell_{\text{comb}} + \ell_{\text{agg}}) + \ell_{\text{read}})^2$ . Thus, the theorem suggests that the VC dimension is  $O(\bar{p}^2 L^2 N^2 d^2)$ , w.r.t. the number parameters  $\bar{p}$  of the GNN, the number of Layers  $L$ , the number  $N$  of graph nodes, and the feature dimension  $d$ . Notice that those meta-parameters are related by constraints, which should be considered in order to understand how VC dimension depends on the

Activation function	Bound	References
Modern GNNs		
Piecewise polynomial	$O(p \log(\mathcal{C}p) + p \log(N))$	[4]
tanh, logsig or atan	$O(p^4 N^2)$	<b>this work</b>
tanh, logsig or atan	$O(p^4 \mathcal{C}^2)$	<b>this work</b>
Original GNNs [22]		
Polynomial	$O(p \log(N))$	[3]
Piecewise polynomial	$O(p^2 N \log(N))$	[3]
tanh, logsig or atan	$O(p^4 N^2)$	[3]
Positional RecNNs		
Polynomial	$O(pN)$	[47]
logsig	$O(p^4 N^2)$	[47]
Sequences (recurrent neural networks)		
Polynomial	$O(pN)$	[48]
Piecewise polynomial	$O(p^2 N)$	[48]
tanh or logsig	$O(p^4 N^2)$	[48]
Vectors (Static multilayer networks)		
Binary	$O(p \log p)$	[49, 50, 51]
Polynomial	$O(p \log p)$	[52]
Piecewise polynomial	$O(p^2)$	[52, 48]
tanh, logsig or atan	$O(p^4)$	[41]

Table 1: Upper bounds on VC-dim of common architectures:  $p$  is the number of the network parameters,  $N$  the number of nodes in the input graph or sequence,  $\mathcal{C}$  the maximum number of colors per graph.

single meta-parameters. Thus, VC dimension is at most  $O(p^4)$ , because when the number  $p$  of parameters grows also the number  $L$  of layers and/or the feature dimension  $d$  grow. Interestingly, such a result is similar to those already obtained for feedforward and recurrent neural networks with Pfaffian activation functions.

Table 1 compares our result with those available in literature. Thus, even if GNNs are more complex, the order of growth of the VC dimension, w.r.t the parameters, is the same of those simple models.

The following theorem clarifies how the VC dimension depends on each meta-parameter.

**Theorem 2.** With respect to the Pfaffian functions  $\text{COMBINE}^{(t)}$ ,  $\text{AGGREGATE}^{(t)}$  and  $\text{READOUT}$  defined in Theorem 1, if  $p_{\text{comb}}, p_{\text{aggr}}, p_{\text{read}} \in \mathcal{O}(d)$  then the

VC dimension of a GNN defined as in Equation (2), w.r.t.  $\bar{p}, H, N, L, d, q$  satisfies

$$\begin{aligned}\text{VCdim}(\text{GNN}) &\leq \mathcal{O}(\bar{p}^4) \\ \text{VCdim}(\text{GNN}) &\leq \mathcal{O}(N^2) \\ \text{VCdim}(\text{GNN}) &\leq \mathcal{O}(L^4) \\ \text{VCdim}(\text{GNN}) &\leq \mathcal{O}(d^6) \\ \text{VCdim}(\text{GNN}) &\leq \mathcal{O}(q^2)\end{aligned}$$

The proof of Theorem 3 adopts the same reasoning used in [41] to derive a bound on the VC dimension of feedforward neural networks with Pfaffian activation functions and in [3] to provide a bound for the first GNN model. Intuitively, the proof is based on the following steps: it is shown that the computation of GNNs on graphs can be represented by a set of equations defined by Pfaffian functions with format  $(\bar{\alpha}, \bar{\beta}, \bar{\ell})$ , where  $\bar{\alpha}, \bar{\beta}, \bar{\ell}$  are those defined in the theorem; then the bound is obtained exploiting a result in [41] that connects the VC dimension with the number of connected components in the inverse images of an system of Pfaffian equations and a result in [53] that allows to estimate the required number of connected components. Notice that our bound and other bounds obtained for networks with Pfaffian activation functions are larger than those for networks with simpler activations. As explained in [41], in [3], such a difference is likely due to the fact that tight bounds are more difficult to achieve with Pfaffian functions and depends on the current general limits of mathematics in the field.

In order to provide a the a specific GNN model, we derive VC-bounds specifically for the architecture described by Eqs. (3) - (5).

**Theorem 3.** Let us consider the GNN model described by Eqs. (3),(5). If  $\sigma$  is a Pfaffian function in  $x$  with format  $(\alpha_\sigma, \beta_\sigma, \ell_\sigma)$  then the VC dimension satisfies

$$\text{VCdim}(\text{GNN}) \leq 2 \log B + \bar{p}(16 + 2 \log \bar{s})$$

where  $B \leq 2^{\frac{\bar{\ell}(\bar{\ell}-1)}{2}+1}(\bar{\alpha} + 2\bar{\beta} - 1)^{\bar{p}-1}((2\bar{p} - 1)(\bar{\alpha} + \bar{\beta}) - 2\bar{p} + 2)^{\bar{\ell}}$ ,  $\bar{\alpha} = 2 + 3\alpha_\sigma$ ,  $\bar{\beta} = \beta_\sigma$ ,  $\bar{\ell} = \bar{p}H\ell_\sigma$ , and  $\bar{s} = LNd + Nq + 1$  holds.

If  $\sigma$  is the logistic sigmoid activation function, we have

$$\begin{aligned}\text{VCdim}(\text{GNN}) &\leq \bar{p}^2 H^2 + 2\bar{p} \log(9) \\ &\quad + 2\bar{p}H \log(16\bar{p}) \\ &\quad + \bar{p}(16 + 2 \log(\bar{s}))\end{aligned}$$

The following theorem shows that the obtained bounds are perfectly coherent with the ones achieved in the general case.

**Theorem 4.** The VC dimension of a GNN defined as in Equation (2), w.r.t.  $\bar{p}, H, N, L, d, q$  satisfies

$$\text{VCdim}(\text{GNN}) \leq \mathcal{O}(\bar{p}^2 H^2)$$

$$\text{VCdim}(\text{GNN}) \leq \mathcal{O}(N^2)$$

$$\text{VCdim}(\text{GNN}) \leq \mathcal{O}(L^4)$$

$$\text{VCdim}(\text{GNN}) \leq \mathcal{O}(d^6)$$

$$\text{VCdim}(\text{GNN}) \leq \mathcal{O}(q^2)$$

## 4.2 Bounds with 1-WL colors

The developed theory is easily adapted to the case when nodes can be grouped according to their colors so as defined by the Weisfeiler-Lehman algorithm. Since, a group of nodes with the same color are computationally equivalent, then the corresponding equations can be merged. Formally, for a given graph  $G$ , let  $C_1(G) = \sum_{i=1}^L C^t(G)$  be the number of colors generated by 1-WL, where  $C^t(G)$  is the number of colors at step  $t > 0$ . Moreover, let us assume that  $C^t(G)$  is bounded in the domain, namely there is  $C_1$  such that  $C_1(G) \leq C_1$  for all the graphs  $G$  in the domain. Similarly, let  $C_0(G)$  be the number of colors of the graph generated by 1-WL at the initial step and assume that there exists  $C_0$  such that  $C_0(G) \leq C_0$  for all the graphs of the domain. The following theorem provides a bound on VC dimension w.r.t. the such numbers of colors.

**Theorem 5.** Assume a subset  $\mathcal{S} \subseteq \mathcal{G}$  and consider a GNN using the logistic sigmoid `logsig` as the activation function. The VC dimension of the GNN satisfies

$$\text{VCdim}(\text{GNN}(C_1)) \leq \mathcal{O}(C_1^2)$$

$$\text{VCdim}(\text{GNN}(C_0)) \leq \mathcal{O}(\log(C_0)).$$

The result suggests that VC dimension depends quadratically on the total number of node colors and logarithmically on the initial number of colors. Actually, a GNN processes all the nodes of a graph at the same time and the GNN architecture is similar to a feedforward network where some computation units are replicated at each node. Thus, the complexity of

GNN growth with the number of nodes and this explains the dependence of the VC dimension on the number of nodes (see Theorem 4). On the other hand, nodes with the same colors cannot be distinguished by the GNN: this means that, in theory, we can use the computation units for a group of nodes sharing the color. Thus, to get tighter bounds on VC dimension we can consider the number of colors in place of the number of nodes. Finally, it is worth mentioning that even if a large the number of nodes/colors for each graph increases the VC dimension of a GNN and, as consequence, decrease its generalization capability, the generalization capability also depends on the number of patterns in training set (see Eqs (6)). In GNNs and graph focused tasks, each graph of the training set is a pattern, but graphs with same sewte of colors have to be considered duplicates; in node focused tasks, the nodes are patterns and the nodes with the same color are duplicates. Thus, the generalization performance of a GNN improves when the total number of graph/node colors in train set increases, in graph/node focused tasks, respectively.

## 5 Experimental validation

In this section, we present an experimental validation of our theoretical results. We will show how the VC dimension of GNNs evolves along with the variation of the parameters respecting the bounds found in Theorems 4 and 5, as in our experimental framework we will exploit the GNN convolution described in Eqs. (3) - (5).

### 5.1 Experimental setting

We design two experimental frameworks to assess the validity, respectively, of Theorems 4 and 5. For both frameworks, we train a Graph Neural Network made by message passing layers defined as in Equation (3), where the activation function  $f$  is either the `arctan` activation function or the `tanh` activation function; the final READOUT layer is made by an affine layer  $W_{\text{out}} \in \mathbb{R}^{\text{hd} \times o}$ , after which a `logsig` activation function is applied; here  $o$  denotes the dimension of the output. The model is trained via Adam optimizer with a learning rate  $\lambda = 10^{-3}$ . The hidden feature size is denoted by `hd` and the number of layers by  $l$ .

**E1:** We measure the evolution of the difference between the train accuracy and the validation accuracy  $\text{diff} = \text{train\_acc} - \text{test\_acc}$  through the training epochs, over three different datasets taken from the TUDataset

repository [54]: PROTEINS, NCI1 and PTCMR. The choice of the datasets has been driven by their binary classification nature. On the first part of the experiment, we fix the hidden features size to  $hd = 32$  and we let the number of layers vary in a certain range, i.e.  $l \in [2, 3, 4, 5, 6]$ , to measure how `diff` evolves. On the second part, we fix the hidden features size to  $l = 3$  and we let the hidden features size vary in a certain range,  $hd \in [8, 16, 32, 64, 128]$ , to perform the same task. We train the model for 500 epochs in each run, with batch size fixed equal to 32.

**E2:** We measure the evolution of the difference between the train accuracy and the validation accuracy  $\text{diff} = \text{train\_acc} - \text{test\_acc}$  through the training epochs over the dataset NCI1, whose graphs are increasingly ordered according to the ratio  $\frac{|V(G)|}{C^t(G)}$ , splitted in 4 different groups. The intuition here is that, being the number of nodes of the graphs bounded, splitting the dataset ordered as said above should provide datasets in which the total number of colors is progressively increasing. Hidden size is fixed as  $hd = 16$ , the number of layers is fixed as  $l = 4$ , the batch size is fixed equal to 32. We report in Table 1 the reference values for each split. We train the model for 2000 epochs (the number of epochs is greater with respect to task **E1** because this task presented greater instability during the training optimization)

	Split 1	Split 2	Split 3	Split 4
# Nodes	27667	30591	31763	32673
# Colors	26243	26569	24489	16348
$\min_G \frac{\#Nodes(G)}{\#Colors(G)}$	1.000	1.105	1.208	1.437
$\max_G \frac{\#Nodes(G)}{\#Colors(G)}$	1.105	1.208	1.437	8

Figure 1: Summary of the parameters for each split of the ordered NCI1 dataset in task **E2**.

Each experiment is statistically evaluated over 10 runs. The overall training is performed on an Intel(R) Core(TM) i7-9800X processor running at 3.80GHz, using 31GB of RAM and a GeForce GTX 1080 Ti GPU unit. The code developed to run the experiments exploits the Python package `PytorchGeometric`; the code can be found at <https://github.com/AleDinve/vc-dim-gnn>.

## 5.2 Experimental results

**Task E1** Numerical results for the NCI1 dataset are reported in Figures 2 and 3. Numerical results for PROTEINS and PTC\_MR datasets are reported in Appendix B.

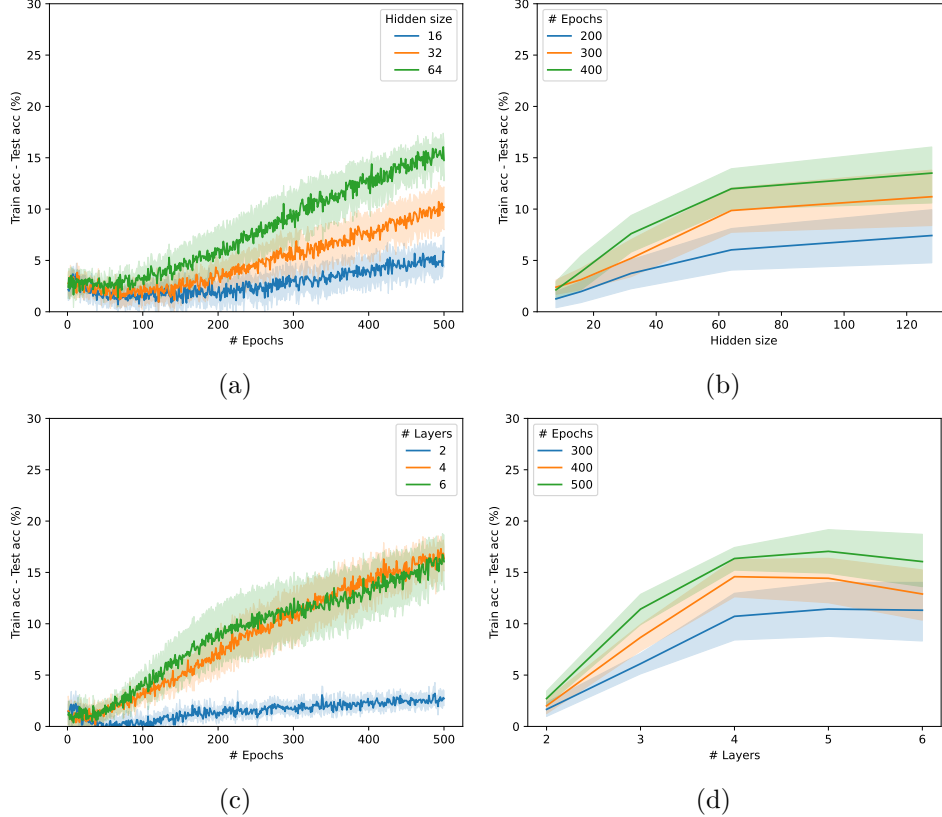


Figure 2: Results on the task **E1** for GNNs with activation function  $\arctan$ . Pictures 2a and 2c show the evolution of diff through the epochs, for certain values of  $hd$  keeping fixed  $l = 3$ , and for certain values of  $l$  keeping fixed  $hd = 32$ ; Picture 2b shows how diff evolves as the hidden size increases, for certain epochs, while Picture 2d shows how diff evolves as the number of layers increases.

The behaviour of the evolution of diff shows coherence to the bounds provided by Theorem 4 with respect to the increase in the hidden size or in the number of layers. Although it is hard to establish a precise function that links the VC dimension to diff, given also the complex nature of the

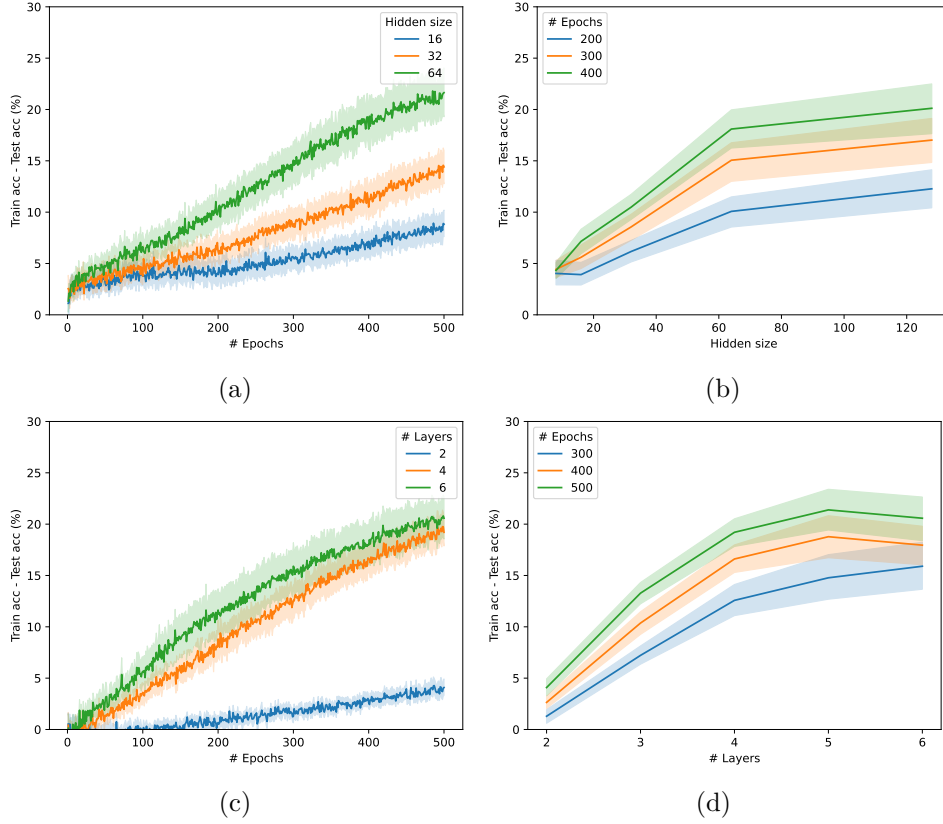


Figure 3: Results on the task **E1** for GNNs with activation function  $\tanh$ . Pictures 3a and 3c show the evolution of  $\text{diff}$  through the epochs, for certain values of  $\text{hd}$  keeping fixed  $l = 3$ , and for certain values of  $l$  keeping fixed  $\text{hd} = 32$ ; Picture 3b shows how  $\text{diff}$  evolves as the hidden size increases, for certain epochs, while Picture 3d shows how  $\text{diff}$  evolves as the number of layers increases.

theoretical framework as the one of the Pfaffian functions, we can partially rely on Equation (6) (which is valid for large sample sets) to argue that our bounds are verified by this experimental setting.

**Task E2** Here, numerical results for the NCI1 dataset are reported in Figure 4.

Similar observations as for experimental setting **E1** can be drawn here: indeed, the evolution of  $\text{diff}$  in our experiment is consistent with the bounds



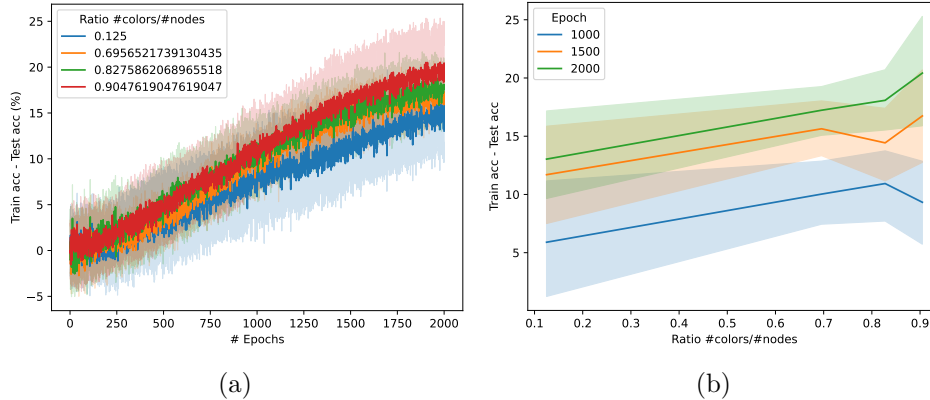


Figure 4: Results on the task **E2** for GNNs with activation function  $\tanh$ . Picture 4a shows the evolution of  $\text{diff}$  through the epochs, for certain values of  $\frac{V(G)}{C^t(G)}$  keeping fixed  $l = 4$  and  $\text{hd} = 16$ ; Picture 4b shows how  $\text{diff}$  evolves as the ratio  $\frac{V(G)}{C^t(G)}$  increases, for certain epochs.

presented in Theorem 5 as the ratio between colors and nodes increases.

## 6 Discussion

In this work we derived new bounds for the VC dimension of modern message passing GNNs with Pfaffian activation functions, closing the gap left in literature with respect to the set of common used activation functions; moreover, we exhibit a preliminar experimental validation to partially show consistency between theory and practice.

Several directions of improvement can be provided: first of all, our work lacks of *lower bounds*, which could give a more precise intuition of the degradation of generalization capabilities for GNNs within the architectural framework here analyzed. In addition, providing a map between the VC dimension and the difference between the training accuracy and the test accuracy would be much more informative; we could establish a quantitative measure with respect to the number of parameters that could allow us to better explain the experimental performances. Finally, it would be interesting to extend the analysis on the VC dimension to other GNN paradigms, such as Graph Transformers [55] and Graph Diffusion Models [56].

## References

- [1] C. Morris, M. Ritzert, M. Fey, W. L. Hamilton, Jan Eric Lenssen, G. Rattan, and M. Grohe. Weisfeiler and leman go neural: Higher-order graph neural networks. In *AAAI Conference on Artificial Intelligence*, pages 4602–4609, 2019.
- [2] K. Xu, W. Hu, J. Leskovec, and S. Jegelka. How powerful are graph neural networks? *International Conference on Machine Learning*, 2019.
- [3] F. Scarselli, A. C. Tsoi, and M. Hagenbuchner. The vapnik-chervonenkis dimension of graph and recursive neural networks. *Neural Networks*, 108:248–259, 2018.
- [4] Christopher Morris, Floris Geerts, Jan Tönshoff, and Martin Grohe. WL meet VC. *Proceedings of the 40th International Conference on Machine Learning*, 2023.
- [5] David Rolnick, Priya L Donti, Lynn H Kaack, Kelly Kochanski, Alexandre Lacoste, Kris Sankaran, Andrew Slavin Ross, Nikola Milojevic-Dupont, Natasha Jaques, Anna Waldman-Brown, et al. Tackling climate change with machine learning. *ACM Computing Surveys (CSUR)*, 55(2):1–96, 2022.
- [6] Stefania Fresca, Andrea Manzoni, Luca Dedè, and Alfio Quarteroni. Deep learning-based reduced order models in cardiac electrophysiology. *PloS one*, 15(10):e0239416, 2020.
- [7] Remi Lam, Alvaro Sanchez-Gonzalez, Matthew Willson, Peter Wirnsberger, Meire Fortunato, Ferran Alet, Suman Ravuri, Timo Ewalds, Zach Eaton-Rosen, Weihua Hu, et al. Learning skillful medium-range global weather forecasting. *Science*, page eadi2336, 2023.
- [8] John Jumper, Richard Evans, Alexander Pritzel, Tim Green, Michael Figurnov, Olaf Ronneberger, Kathryn Tunyasuvunakool, Russ Bates, Augustin Žídek, Anna Potapenko, et al. Highly accurate protein structure prediction with alphafold. *Nature*, 596(7873):583–589, 2021.
- [9] Kurt Hornik, Maxwell Stinchcombe, and Halbert White. Multilayer feedforward networks are universal approximators. *Neural networks*, 2(5):359–366, 1989.
- [10] Kurt Hornik. Approximation capabilities of multilayer feedforward networks. *Neural networks*, 4(2):251–257, 1991.

- [11] Barbara Hammer. On the approximation capability of recurrent neural networks. *Neurocomputing*, 31(1-4):107–123, 2000.
- [12] Ingrid Daubechies, Ronald DeVore, Simon Foucart, Boris Hanin, and Guergana Petrova. Nonlinear approximation and (deep) relu networks. *Constructive Approximation*, 55(1):127–172, 2022.
- [13] Simone Brugiapaglia, Matthew Liu, and Paul Tupper. Generalizing outside the training set: When can neural networks learn identity effects? *arXiv preprint arXiv:2005.04330*, 2020.
- [14] Simone Brugiapaglia, M Liu, and Paul Tupper. Invariance, encodings, and generalization: learning identity effects with neural networks. *Neural Computation*, 34(8):1756–1789, 2022.
- [15] Giuseppe Alessio D’Inverno, Simone Brugiapaglia, and Mirco Ravanelli. Generalization limits of graph neural networks in identity effects learning. *arXiv preprint arXiv:2307.00134*, 2023.
- [16] Arthur Jacot, Franck Gabriel, and Clément Hongler. Neural tangent kernel: Convergence and generalization in neural networks. *Advances in neural information processing systems*, 31, 2018.
- [17] Behnam Neyshabur, Zhiyuan Li, Srinadh Bhojanapalli, Yann LeCun, and Nathan Srebro. Towards understanding the role of over-parametrization in generalization of neural networks. *arXiv preprint arXiv:1805.12076*, 2018.
- [18] Vladimir Koltchinskii. Rademacher penalties and structural risk minimization. *IEEE Transactions on Information Theory*, 47(5):1902–1914, 2001.
- [19] David Haussler and Manfred Warmuth. The probably approximately correct (PAC) and other learning models. *The Mathematics of Generalization*, pages 17–36, 2018.
- [20] Vladimir N Vapnik and A Ya Chervonenkis. On the uniform convergence of relative frequencies of events to their probabilities. In *Doklady Akademii Nauk USSR*, volume 181, pages 781–787, 1968.
- [21] Vladimir Vapnik. *Estimation of dependences based on empirical data*. Springer Science & Business Media, 2006.

- [22] F. Scarselli, M. Gori, A. C. Tsoi, M. Hagenbuchner, and G. Monfardini. The graph neural network model. *IEEE Transactions on Neural Networks*, 20(1):61–80, 2009.
- [23] Jie Zhou, Ganqu Cui, Shengding Hu, Zhengyan Zhang, Cheng Yang, Zhiyuan Liu, Lifeng Wang, Changcheng Li, and Maosong Sun. Graph neural networks: A review of methods and applications. *AI open*, 1:57–81, 2020.
- [24] Zhiyuan Liu and Jie Zhou. *Introduction to graph neural networks*. Springer Nature, 2022.
- [25] B. Weisfeiler and A. Leman. The reduction of a graph to canonical form and the algebra which appears therein. *Nauchno-Technicheskaya Informatsia*, 2(9):12–16, 1968. English translation by G. Ryabov is available at [https://www.iti.zcu.cz/wl2018/pdf/wl\\_paper\\_translation.pdf](https://www.iti.zcu.cz/wl2018/pdf/wl_paper_translation.pdf).
- [26] Cristian Bodnar, Fabrizio Frasca, Yuguang Wang, Nina Otter, Guido F Montufar, Pietro Lio, and Michael Bronstein. Weisfeiler and Lehman Go Topological: Message Passing Simplicial Networks. In *International Conference on Machine Learning*, pages 1026–1037. PMLR, 2021.
- [27] Cristian Bodnar, Fabrizio Frasca, Nina Otter, Yuguang Wang, Pietro Lio, Guido F Montufar, and Michael Bronstein. Weisfeiler and lehman go cellular: Cw networks. *Advances in Neural Information Processing Systems*, 34:2625–2640, 2021.
- [28] Vikas Garg, Stefanie Jegelka, and Tommi Jaakkola. Generalization and representational limits of graph neural networks. In *International Conference on Machine Learning*, pages 3419–3430. PMLR, 2020.
- [29] Andreas Krebs and Oleg Verbitsky. Universal covers, color refinement, and two-variable counting logic: Lower bounds for the depth. In *2015 30th Annual ACM/IEEE Symposium on Logic in Computer Science*, pages 689–700. IEEE, 2015.
- [30] Giuseppe Alessio D’Inverno, Monica Bianchini, Maria Lucia Sampoli, and Franco Scarselli. On the approximation capability of GNNs in node classification/regression tasks. *arXiv preprint arXiv:2106.08992*, 2021.
- [31] Pascal Esser, Leena Chennuru Vankadara, and Debarghya Ghoshdastidar. Learning theory can (sometimes) explain generalisation in graph neural networks. *Advances in Neural Information Processing Systems*, 34:27043–27056, 2021.

- [32] Saurabh Verma and Zhi-Li Zhang. Stability and generalization of graph convolutional neural networks. In *Proceedings of the 25th ACM SIGKDD International Conference on Knowledge Discovery & Data Mining*, pages 1539–1548, 2019.
- [33] Renjie Liao, Raquel Urtasun, and Richard Zemel. A PAC-bayesian approach to generalization bounds for Graph Neural Networks. *arXiv preprint arXiv:2012.07690*, 2020.
- [34] Haotian Ju, Dongyue Li, Aneesh Sharma, and Hongyang R Zhang. Generalization in Graph Neural Networks: Improved PAC-Bayesian bounds on graph diffusion. In *International Conference on Artificial Intelligence and Statistics*, pages 6314–6341. PMLR, 2023.
- [35] Boris Knyazev, Graham W Taylor, and Mohamed Amer. Understanding attention and generalization in graph neural networks. *Advances in neural information processing systems*, 32, 2019.
- [36] Vladimir Vapnik, Esther Levin, and Yann Le Cun. Measuring the vc-dimension of a learning machine. *Neural computation*, 6(5):851–876, 1994.
- [37] Eduardo D Sontag et al. Vc dimension of neural networks. *NATO ASI Series F Computer and Systems Sciences*, 168:69–96, 1998.
- [38] Peter L Bartlett and Wolfgang Maass. Vapnik-chervonenkis dimension of neural nets. *The handbook of brain theory and neural networks*, pages 1188–1192, 2003.
- [39] Pascal Koiran and Eduardo D Sontag. Vapnik-chervonenkis dimension of recurrent neural networks. *Discrete Applied Mathematics*, 86(1):63–79, 1998.
- [40] Askold G Khovanski. *Fewnomials*, volume 88. American Mathematical Soc., 1991.
- [41] Marek Karpinski and Angus Macintyre. Polynomial bounds for VC dimension of sigmoidal and general pfaffian neural networks. *J. Comput. Syst. Sci.*, 54(1):169–176, 1997.
- [42] Monica Bianchini and Franco Scarselli. On the complexity of neural network classifiers: A comparison between shallow and deep architectures. *IEEE transactions on neural networks and learning systems*, 25(8):1553–1565, 2014.

- [43] Sandra Kiefer. The Weisfeiler-Leman algorithm: an exploration of its power. *ACM SIGLOG News*, 7(3):5–27, 2020.
- [44] Will Hamilton, Zhitao Ying, and Jure Leskovec. Inductive representation learning on large graphs. *Advances in Neural Information Processing Systems*, 30, 2017.
- [45] Thomas N Kipf and Max Welling. Semi-supervised classification with graph convolutional networks. *arXiv preprint arXiv:1609.02907*, 2016.
- [46] VN Vapnik and A Ya Chervonenkis. On the uniform convergence of relative frequencies of events to their probabilities. *Theory of Probability & Its Applications*, 16(2):264–280, 1971.
- [47] Barbara Hammer. On the generalization ability of recurrent networks. In *Artificial Neural Networks—ICANN 2001: International Conference Vienna, Austria, August 21–25, 2001 Proceedings 11*, pages 731–736. Springer, 2001.
- [48] Pascal Koiran and Eduardo D Sontag. Neural networks with quadratic vc dimension. *journal of computer and system sciences*, 54(1):190–198, 1997.
- [49] Eric Baum and David Haussler. What size net gives valid generalization? *Advances in neural information processing systems*, 1, 1988.
- [50] Wolfgang Maass. Neural nets with superlinear vc-dimension. *Neural Computation*, 6(5):877–884, 1994.
- [51] Akito Sakurai. On the vc-dimension of depth four threshold circuits and the complexity of boolean-valued functions. *Theoretical computer science*, 137(1):109–127, 1995.
- [52] Paul Goldberg and Mark Jerrum. Bounding the vapnik-chervonenkis dimension of concept classes parameterized by real numbers. In *Proceedings of the sixth annual conference on Computational learning theory*, pages 361–369, 1993.
- [53] Andrei Gabrielov and Nicolai Vorobjov. Complexity of computations with pfaffian and noetherian functions. *Normal forms, bifurcations and finiteness problems in differential equations*, 137:211–250, 2004.

- [54] Christopher Morris, Nils M. Kriege, Franka Bause, Kristian Kersting, Petra Mutzel, and Marion Neumann. Tudataset: A collection of benchmark datasets for learning with graphs. In *ICML 2020 Workshop on Graph Representation Learning and Beyond (GRL+ 2020)*, 2020.
- [55] Seongjun Yun, Minbyul Jeong, Raehyun Kim, Jaewoo Kang, and Hyunwoo J Kim. Graph transformer networks. *Advances in neural information processing systems*, 32, 2019.
- [56] Mengchun Zhang, Maryam Qamar, Taegoo Kang, Yuna Jung, Chen-shuang Zhang, Sung-Ho Bae, and Chaoning Zhang. A survey on graph diffusion models: Generative ai in science for molecule, protein and material. *arXiv preprint arXiv:2304.01565*, 2023.
- [57] Andrei Gabrielov and Nicolai Vorobjov. Complexity of stratification of semi-pfaffian sets. *Discrete & computational geometry*, 14(1):71–91, 1995.

## A Proof of main results

In order to to introduce the main idea exploited to prove Theorem 4 in details, we have to recall the main notation and results from [41].

### A.1 Results from literature

#### Representing the computation of a neural network by a set of Pfaffian equations

Let  $\tau_1, \dots, \tau_{\bar{s}}$  be a set of  $C^\infty$  infinitely differentiable functions from  $\mathbb{R}^{p+\gamma}$  to  $\mathbb{R}$ . Suppose that  $\Phi(\mathbf{y}, \theta)$ ,  $\mathbf{y} \in \mathbb{R}^\gamma$ ,  $\theta \in \mathbb{R}^p$  is a quantifier-free logical formula constructed using the logical "and" and atoms in the form of  $\tau_i(\mathbf{y}, \theta) = 0$ . Note that, fixed  $\theta$ ,  $\Phi(\cdot, \theta)$  takes as input a vector  $\mathbf{y}$  and returns a logical value, so that it can be used as a classifier with input  $\mathbf{y}$  and parameters  $\theta$ . Later, we will see that  $\tau_1, \dots, \tau_{\bar{s}}$  can be specified so that  $\Phi(\cdot, \theta)$  defines the computation of a GNN. Moreover, its VC-dim can be easily defined. In fact,  $\Phi$  is said to shatter a set  $\mathcal{S} = \{\bar{\mathbf{y}}_1, \dots, \bar{\mathbf{y}}_r\}$  if for any set of binary assignments  $\delta = [\delta_1, \dots, \delta_r] \in \{0, 1\}^r$ , there exist parameters  $\bar{\theta}$  such that, for any  $i$ ,  $\Phi(\mathbf{y}_i, \bar{\theta})$  is true if  $\delta_i = 1$ , and  $\Phi(\mathbf{y}_i, \bar{\theta})$  is false if  $\delta_i = 0$ . Then, the VC-dim of  $\Phi$  is defined as the size of the maximum set that  $\Phi$  can shatter, i.e.,

$$\text{VCdim}(\Phi) = \max_{\mathcal{S} \text{ is shattered by } \Phi} |\mathcal{S}|$$

### The VCdim of a network and the number of connected components of the inverse images of the Pfaffian functions

Interestingly, it can be shown that the VC dimension of  $\Phi(\cdot, \theta)$  can be studied by analysing the topological properties of the inverse image of the components of  $\Phi(\mathbf{y}, \cdot)$  for every input  $\mathbf{y}$ . More precisely, let  $\bar{y}_1, \dots, \bar{y}_z$  be vectors in  $\mathbb{R}^{\bar{\gamma}}$ , and  $T : \mathbb{R}^{\bar{p}} \rightarrow \mathbb{R}^{\bar{u}}$ ,  $\bar{u} \leq \bar{p}$ , be defined as

$$T(\bar{\theta}) = [\bar{\tau}_1(\bar{\theta}), \dots, \bar{\tau}_{\bar{u}}(\bar{\theta})], \quad (7)$$

where  $\bar{\tau}_1(\bar{\theta}), \dots, \bar{\tau}_{\bar{u}}(\bar{\theta})$  are functions chosen from those in the form of  $\tau_i(\bar{\mathbf{y}}_j, \bar{\theta})$ , i.e., for each  $r$ ,  $1 \leq r \leq \bar{u}$  there exist integers  $i$  and  $j$  such that  $\bar{\tau}_r(\bar{\theta}) = \tau_i(\bar{\mathbf{y}}_j, \bar{\theta})$ . Let  $[\epsilon_1, \dots, \epsilon_{\bar{u}}]$  be a regular value of  $T^1$  and assume that there exists a positive integer  $B$  that bounds the number of connected components of  $T^{-1}(\epsilon_1, \dots, \epsilon_{\bar{u}})$  and does not depend on the chosen  $\epsilon_1, \dots, \epsilon_{\bar{u}}$  and on the  $\bar{\mathbf{y}}_j$  selected to be contained in the  $\bar{\tau}_i$ . Then, the following theorem holds ([41]).

**Theorem 6** ([41]). The VC-dim of  $\Phi$  is bounded as follows:

$$\text{VCdim}(\Phi) \leq 2 \log B + \bar{p}(16 + 2 \log \bar{s}).$$

The theorem provides VCdim bound that depends: on the number  $\bar{p}$  of parameters; on the total number  $\bar{s}$  of functions  $\tau_i$ ; on  $B$ , which may further depend on the number of parameters.

### Bounds on number of connected components

Then, a bound on  $B$  can be obtained from results in literature. The following results provide a bound for equations of Pfaffian functions.

**Theorem 7** ([53]). Consider a system of equations  $\bar{q}_1(\theta) = 0, \dots, \bar{q}_k(\theta) = 0$ , where  $\bar{q}_i$ ,  $1 \leq i \leq k$ , are Pfaffian functions in a domain  $G \subseteq \mathbb{R}^{\bar{p}}$ , having a common Pfaffian chain of length  $\bar{\ell}$  and maximum degrees  $(\bar{\alpha}, \bar{\beta})$ . Then the number of connected components of the set  $\{\theta | \bar{q}_1(\theta) = 0, \dots, \bar{q}_k(\theta) = 0\}$  is bounded by

$$2^{\frac{\bar{\ell}(\bar{\ell}-1)}{2}+1}(\bar{\alpha} + 2\bar{\beta} - 1)^{\bar{p}-1}((2\bar{p} - 1)(\bar{\alpha} + \bar{\beta}) - 2\bar{p} + 2)^{\bar{\ell}}$$

<sup>1</sup>We recall that  $[\epsilon_1, \dots, \epsilon_{\bar{u}}]$  is a regular value of  $T$  if either  $T^{-1}([\epsilon_1, \dots, \epsilon_{\bar{u}}]) = \emptyset$  or  $T^{-1}([\epsilon_1, \dots, \epsilon_{\bar{u}}])$  is an  $(\bar{p} - \bar{u})$ -dimensional  $C^\infty$ -submanifold of  $\mathbb{R}^{\bar{p}}$



## A.2 Proof of Theorem 2

### A.2.1 Representing the computation of a neural network by a set of Pfaffian equations - general case

The first step of the proof consists of defining a set of equations  $\tau_i(\mathbf{y}, \theta) = 0$  that specifies the computation of a GNN. Obviously,  $\theta$  includes just the GNN parameters, namely  $\theta = \Theta$ . If  $\text{COMBINE}^{(t)}$  has  $p_{\text{comb}}$  parameters for  $1 \leq t \leq L$ ,  $\text{AGGREGATE}^{(t)}$  has  $p_{\text{agg}}$  parameters for  $1 \leq t \leq L$  and  $\text{READOUT}$  has  $p_{\text{read}}$  parameters, the total number of parameters is  $L(p_{\text{comb}} + p_{\text{agg}}) + p_{\text{read}}$ .

Moreover, intuitively  $\mathbf{y}$  represents the input of a GNN, so that for a given graph  $\mathbf{G} = (G, \mathbf{L})$  in  $\mathcal{G}$  each  $\mathbf{y}$  contains some vectorial representation of  $\mathbf{G}$ , namely the  $Nq$  graph attributes in  $\mathbf{L}$  and a vectorial representation of the adjacency matrix, which requires  $N(N-1)/2$  elements.

Furthermore, to define the equations, we use the same trick as in [41] and we introduce new variables for each computation unit of the network. Those variables belongs to the input  $\mathbf{y}$  of  $\tau$ . More precisely, we consider a vector of  $d$  variables  $h_v^{(t)}$  for each node  $v$  and for each layer  $t$ . Notice, since we may be interested in defining more computations of the GNN on more graphs at the same time, here  $v$  implicitly addresses a specific node of some graph in the domain. Finally, a variable  $\text{READOUT}$  for each graph and contains just a single output of the GNN. In total, the dimension of  $\mathbf{y}$  is  $\bar{p} = Nq + N(N-1)/2 + NdL + 1$ .

Then, by (2), the computation of GNN is straightforwardly defined by the following set of  $LNd + Nq + 1$  equations,

$$h_v^{(0)} - \mathbf{L}_v = 0 \quad (8)$$

$$h_v^{(t)} - \text{COMBINE}^{(t+1)}(h_v^{(t)}, \text{AGGREGATE}^{(t+1)}(\{\{h_u^{(t)} | u \in \text{ne}(v)\}, A\})) = 0 \quad (9)$$

$$\overline{\text{READOUT}} - \text{READOUT}(\{h_v^{(L)} : v \in V\}) = 0 \quad (10)$$

where  $A$  is the variable storing the adjacency matrix of the input graph. We can assume that  $A$  is valid for every graph in the domain if the domain is made by finite graphs.

### A.2.2 The format of the Pfaffian functions - general case

The following lemma specifies the format of Pfaffian functions involved in the above equations.

**Lemma 8.** Let  $\text{COMBINE}^{(t)}$ ,  $\text{AGGREGATE}^{(t)}$  and  $\text{READOUT}$  be Pfaffian functions with format, respectively,  $(\alpha_{\text{comb}}, \beta_{\text{comb}}, \ell_{\text{comb}})$ ,  $(\alpha_{\text{agg}}, \beta_{\text{agg}}, \ell_{\text{agg}})$ ,  $(\alpha_{\text{read}}, \beta_{\text{read}}, \ell_{\text{read}})$  w.r.t. the variables  $\mathbf{y}$  and  $\mathbf{w}$  described above,

1. the left part of Equation (8) is a polynomial of degree 1;
2. the left part of Equation (9) is a Pfaffian function having format  $(\alpha_{\text{agg}} + \beta_{\text{agg}} - 1 + \alpha_{\text{comb}}\beta_{\text{agg}}, \beta_{\text{comb}}, \ell_{\text{comb}} + \ell_{\text{agg}})$ ;
3. the left part of Equation (10) is a Pfaffian function having format  $(\alpha_{\text{read}}, \beta_{\text{read}}, \ell_{\text{read}})$ ;
4. Equations (8)-(10) constitutes a system of Pfaffian equations with format  $(\alpha_{\text{system}}, \beta_{\text{system}}, LNd(\ell_{\text{comb}} + \ell_{\text{agg}}) + \ell_{\text{read}})$ , where  $\alpha_{\text{system}} = \max\{\alpha_{\text{agg}}, \alpha_{\text{comb}}, \alpha_{\text{read}}\}$ ,  $\beta_{\text{system}} = \max\{\beta_{\text{comb}}, \beta_{\text{read}}\}$  and the shared chain is obtained by concatenating the chains of Equations (9),(10).

*Proof.* The first point is straightforward. The second and third points can be derived by applying the composition lemma for Pfaffian functions [57], according to which if two functions  $f$  and  $g$  have format  $(\alpha_f, \beta_f, \ell_f)$  and  $(\alpha_g, \beta_g, \ell_g)$ , respectively, then their composition  $f \circ g$  has format  $(\alpha_g + \beta_g - 1 + \alpha_f\beta_g, \beta_f, \ell_f + \ell_g)$ .

Finally, the fourth point is a consequence of the fact that the equations are independent and the chains can be concatenated. The length of the chain is obvious consequence of the fact that there are  $H = LNd$  equations involving both COMBINE and AGGREGATE and one equation involving READOUT. The degree is obtained taking the largest degree of a Pfaffian function.  $\square$

### Bounding the number $B$ of connected components

Thus, according to the discussion in Section A.1, we have a bound on the number of connected components on the inverse image of the function  $T$  of Equation (7). In our case,  $T$  is defined by a subset containing  $\bar{u}$  equations from those in (8), (9), (10).

Intuitively, according to Equations (7), the  $i$ -th equation of the subset is focused on an input pattern  $\mathbf{y}_i$ , which in our case corresponds to a graph and some input attributes, and on the value of a GNN variable.

Thus, the following lemma follows directly by applying Theorem 7.

**Lemma 9.** The number  $B$  of connected components satisfies

$$B \leq 2^{\frac{\bar{\ell}(\bar{\ell}-1)}{2}+1}(\bar{\alpha} + 2\bar{\beta} - 1)^{\bar{p}-1}((2\bar{p} - 1)(\bar{\alpha} + \bar{\beta}) - 2\bar{p} + 2)^{\bar{\ell}}$$

where  $\bar{p} = L(p_{\text{comb}} + p_{\text{agg}}) + p_{\text{read}}$ ,  $\bar{\alpha} = \alpha_{\text{system}}$ ,  $\bar{\beta} = \beta_{\text{system}}$ ,  $\bar{\ell} = \bar{p}(LNd(\ell_{\text{comb}} + \ell_{\text{agg}}) + \ell_{\text{read}})$ .

### A bound on VC dimension

Finally, by Theorem 6, the bound on the VC dimension is derived.

**Lemma 10.** The VC dimension of GNN described by Equations (8)-(10) is bounded by

$$\text{VCdim}(\Phi) \leq 2 \log B + \bar{p}(16 + 2 \log \bar{s}).$$

where  $\bar{p} = L(p_{\text{comb}} + p_{\text{agg}}) + p_{\text{read}}$ ,  $\bar{s} = LNd + Nq + 1$  hold.

Thus, we can finally bound the VC dimension a GNN in the general case.

**Proposition 11.** Let us assume that  $\alpha_{\text{system}}, \beta_{\text{system}} \leq \gamma$  for a constant  $\gamma \in \mathbb{R}$  in Lemma 8. Then, the VC dimension of a GNN as defined by Equations (8)-(10) is bounded by

$$\begin{aligned} \text{VCdim}(\text{GNN}) &\leq (L(p_{\text{comb}} + p_{\text{agg}}) + p_{\text{read}})^2 (LNd(\ell_{\text{comb}} + \ell_{\text{agg}}) + \ell_{\text{read}}))^2 \\ &\quad + 2(L(p_{\text{comb}} + p_{\text{agg}}) + p_{\text{read}}) \log(3\gamma) \\ &\quad + 2(L(p_{\text{comb}} + p_{\text{agg}}) + p_{\text{read}}) \log((4\gamma - 2)(L(p_{\text{comb}} + p_{\text{agg}}) + p_{\text{read}} + 2 - 2\gamma)) \\ &\quad + (L(p_{\text{comb}} + p_{\text{agg}}) + p_{\text{read}})(16 + 2 \log(LNd + Nq + 1)), \end{aligned}$$

The initial assumption of this Proposition is usually met, as  $\alpha_{\text{system}}$  and  $\beta_{\text{system}}$  depends only on the selected activation function in the network.

*Proof.* From Lemmas 7 and 9, we have

$$\begin{aligned} \text{VCdim}(\text{GNN}) &\leq 2 \log B + \bar{p}(16 + 2 \log \bar{s}) \\ &\leq 2 \log \left( 2^{\frac{\bar{\ell}(\bar{\ell}-1)}{2}+1} (\bar{\alpha} + 2\bar{\beta} - 1)^{\bar{p}-1} ((2\bar{p} - 1)(\bar{\alpha} + \bar{\beta}) - 2\bar{p} + 2)^{\bar{\ell}} \right) + \bar{p}(16 + 2 \log \bar{s}) \\ &= \bar{\ell}(\bar{\ell} - 1) + 2(\bar{p} - 1) \log(\bar{\alpha} + 2\bar{\beta} - 1) + 2\bar{\ell} \log((2\bar{p} - 1)(\bar{\alpha} + \bar{\beta}) - 2\bar{p} + 2) \\ &\quad + \bar{p}(16 + 2 \log \bar{s}) + 2 \end{aligned}$$

If we denote  $H = LNd(\ell_{\text{comb}} + \ell_{\text{agg}}) + \ell_{\text{read}}$  we have:

$$\begin{aligned} \text{VCdim}(\text{GNN}) &\leq \bar{p}H(\bar{p}H - 1) + 2(\bar{p} - 1) \log(\alpha_{\text{system}} + 2\beta_{\text{system}} - 1) \\ &\quad + 2\bar{p}H \log((2\bar{p} - 1)(\alpha_{\text{system}} + \beta_{\text{system}}) - 2\bar{p} + 2) \\ &\quad + \bar{p}(16 + 2 \log(\bar{s})) + 2 \\ &\leq \bar{p}^2 H^2 + 2\bar{p} \log(3\gamma) \\ &\quad + 2\bar{p}H \log((4\gamma - 2)\bar{p} + 2 - 2\gamma) \\ &\quad + \bar{p}(16 + 2 \log(\bar{s})) + 2 \end{aligned}$$

Let's recall that:

$$H = LNd(\ell_{\text{comb}} + \ell_{\text{agg}}) + \ell_{\text{read}}$$

$$\bar{p} = L(p_{\text{comb}} + p_{\text{agg}}) + p_{\text{read}}$$

$$\bar{s} = LNd + Nq + 1$$

Then, by replacing  $\bar{p}$ ,  $H$  and  $\bar{s}$ , it follows

$$\begin{aligned} \text{VCdim}(\text{GNN}) &\leq (L(p_{\text{comb}} + p_{\text{agg}}) + p_{\text{read}})^2 (LNd(\ell_{\text{comb}} + \ell_{\text{agg}}) + \ell_{\text{read}})^2 \\ &\quad + 2(L(p_{\text{comb}} + p_{\text{agg}}) + p_{\text{read}}) \log(3\gamma) \\ &\quad + 2(L(p_{\text{comb}} + p_{\text{agg}}) + p_{\text{read}}) \log((4\gamma - 2)(L(p_{\text{comb}} + p_{\text{agg}}) + p_{\text{read}} + 2 - 2\gamma)) \\ &\quad + (L(p_{\text{comb}} + p_{\text{agg}}) + p_{\text{read}})(16 + 2 \log(LNd + Nq + 1)), \end{aligned}$$

which leads to the thesis.  $\square$

On the base of the above theorem, we can derive the orders of growth of the VC dimension w.r.t. the dimension of the features, the number of the layers and the graph dimension, obtaining Theorem 2.

### A.3 Proof of Theorem 4

Given a attributed graph domain  $\mathcal{G}$ , containing graphs up to  $N$  nodes and whose attributes have dimension  $q$ , we consider the let a GNN be defined by the following updating scheme:

$$h_v^{(t+1)} = \sigma(\mathbf{W}_{\text{comb}}^{(t+1)} h_v^{(t)} + \mathbf{W}_{\text{agg}}^{(t+1)} h_{\mathcal{N}(v)}^{(t+1)} + \mathbf{b}^{(t+1)}) \quad (11)$$

where  $\sigma$  is the activation function and

$$h_{\mathcal{N}(v)}^{(t+1)} = \sum_{u \in \text{ne}(v)} h_u^{(t)} \quad (12)$$

The hidden states are initialised as  $h_v^{(0)} = \mathbf{L}_v$ .

### Representing the computation of a neural network by a set of Pfaffian equations

The first step of the proof consists of defining a set of equations  $\tau_i(\mathbf{y}, \theta) = 0$  that specifies the computation of a GNN. Obviously,  $\theta$  includes just the GNN parameters, namely  $\theta = \Theta$ . It is easily seen that the total number of parameters is  $p = (2d + 1)(d(L - 1) + q + 1) - q$ . Indeed, the parameters are:

- $\mathbf{W}_{\text{comb}}^{(1)}, \mathbf{W}_{\text{agg}}^{(1)} \in \mathbb{R}^{q \times d}, \mathbf{b}^{(1)} \in \mathbb{R}^{1 \times d}$ , so we have  $2dq + d$  parameters;

- $\mathbf{W}_{\text{comb}}^{(t)}, \mathbf{W}_{\text{agg}}^{(t)} \in \mathbb{R}^{d \times d}, \mathbf{b}^{(t)} \in \mathbb{R}^{1 \times d}$  for  $t = 2, \dots, L$ , so we have  $(2d^2 + d)(L - 1)$  parameters;
- $w \in \mathbb{R}^{d \times 1}, b \in \mathbb{R}$ ; we have  $d + 1$  parameters;

So, in the end, we will have  $2dq + d + (2d^2 + d)(L - 1) + d + 1 = (2d + 1)(d(L - 1) + q + 1) - q$  parameters.

Moreover, intuitively  $\mathbf{y}$  represents the input of a GNN, so that for a given graph  $\mathbf{G} = (G, \mathbf{L})$  in  $\mathcal{G}$  each  $\mathbf{y}$  contains some vectorial representation of  $\mathbf{G}$ , namely the  $Nq$  graph attributes in  $\mathbf{L}$  and a vectorial representation of the adjacency matrix, which requires  $N(N - 1)/2$  elements.

Furthermore, to define the equations, we use the same trick as in [41] and we introduce new variables for each computation unit of the network. Those variables belongs to the input  $\mathbf{y}$  of  $\tau$ . More precisely, we consider a vector of  $d$  variables  $h_v^{(t)}$  for each node  $v$  and for each layer  $t$ . Notice, since we may be interested in defining more computations of the GNN on more graphs at the same time, here  $v$  implicitly addresses a specific node of some graph in the domain. Finally, a variable READOUT for each graph and contains just a single output of the GNN. In total, the dimension of  $\mathbf{y}$  is  $Nq + N(N - 1)/2 + NdL + 1$ .

Then, by (11), the computation of GNN is straightforwardly defined by the following set of  $LNd + Nq + 1$  equations,

$$h_{v\cdot}^{(0)} - \mathbf{L}_{v\cdot} = 0 \quad (13)$$

$$h_{v\cdot}^{(t)} - \sigma\left(h_{v\cdot}^{(t-1)}\mathbf{W}_{\text{comb}}^{(t)} + \sum_u h_{u\cdot}^{(t-1)}\mathbf{W}_{\text{agg}}^{(t)}m_{v,u} + \mathbf{b}^{(t)}\right) = 0, \quad (14)$$

$$\text{READOUT} - \sigma\left(\sum_{v \in V} h_{v\cdot}^{(L)}\mathbf{W} + b\right) = 0, \quad (15)$$

where  $m_{v,u}$  is a binary value, which is 1 when  $v$  and  $u$  are connected and 0, otherwise.

### The format of the Pfaffian functions

The following lemma specifies the format of Pfaffian functions involved in the above equations.

**Lemma 12.** Let  $\sigma$  be a Pfaffian function in  $x$  with format  $(\alpha_\sigma, \beta_\sigma, \ell_\sigma)$ , then w.r.t. the variables  $\mathbf{y}$  and  $\mathbf{w}$  described above,

1. the left part of Equation (13) is a polynomial of degree 1;
2. the left part of Equation (14) is a Pfaffian function having format  $(2 + 3\alpha_\sigma, \beta_\sigma, \ell_\sigma)$ ;

3. the left part of Equation (15) is a Pfaffian function having format  $(1 + 2\alpha_\sigma, \beta_\sigma, \ell_\sigma)$ ;
4. Equations (13)-(15) constitutes a system of Pfaffian equations with format  $(2 + 3\alpha_\sigma, \beta_\sigma, H\ell_\sigma)$ , where the shared chain is obtained by concatenating the chains of  $H = LNd + 1$  equations in (14),(15) that includes an activation function.

*Proof.* The first point is straightforward. The second and third points can be derived by applying the composition lemma for Pfaffian functions. Actually, the formula inside  $\sigma$  in Equation (14) is a polynomial of degree 3, due to the factors  $h_u^{(t-1)} \mathbf{W}_{\text{agg}}^{(t)} m_{v,u}$ , while formula inside  $\sigma$  in Equation (15) is a polynomial of degree 2, due to the factors  $h_v^{(L)} \mathbf{W}$ . Moreover, polynomials are Pfaffian functions with null chains,  $\alpha$  equal to 0 and  $\beta$  equals to their degrees. Thus, the functions inside the  $\sigma$  in Equations (14) and (15) have format  $(0, 3, 0)$  and  $(0, 2, 0)$ , respectively. Then, the thesis follows by composition lemma [57], according to which if two functions  $f$  and  $g$  have format  $(\alpha_f, \beta_f, \ell_f)$  and  $(\alpha_g, \beta_g, \ell_g)$ , respectively, then their composition  $f \circ g$  has format  $(\alpha_g + \beta_f - 1 + \alpha_f \beta_g, \beta_f, \ell_f + \ell_g)$ .

Finally, the fourth point is a consequence of the fact that the equations are independent and the chains can be concatenated. The length of the chain is obvious consequence of the fact that there are  $H = LNd + 1$  equations using  $\sigma$ . The degree is obtained copying the largest degree of a Pfaffian function, which is the one in Equation (14).  $\square$

### Bounding the number $B$ of connected components

Thus, according to the discussion in Section A.1, we have a bound on the number of connected components on the inverse image of the function  $T$  of Equation (7). In our case,  $T$  is defined by a subset containing  $\bar{u}$  equations from those in (13), (14), (15).

Intuitively, according to Equations (7), the  $i$ -th equation of the subset is focused on an input pattern  $\mathbf{y}_i$ , which in our case corresponds to a graph and some input attributes, and on the value of a GNN variable.

Thus, the following lemma follows directly by applying Theorem 7.

**Lemma 13.** The number  $B$  of connected components satisfies

$$B \leq 2^{\frac{\bar{\ell}(\bar{\ell}-1)}{2}+1} (\bar{\alpha} + 2\bar{\beta} - 1)^{\bar{p}-1} ((2\bar{p} - 1)(\bar{\alpha} + \bar{\beta}) - 2\bar{p} + 2)^{\bar{\ell}}$$

where  $\bar{p} = (2d + 1)(d(L - 1) + q + 1) - q$ ,  $\bar{\alpha} = 2 + 3\alpha_\sigma$ ,  $\bar{\beta} = \beta_\sigma$ ,  $\bar{\ell} = \bar{p}H\ell_\sigma$ .

## A bound on VC dimension

Finally, by Theorem 6, the bound on the VC dimension is derived.

**Lemma 14.** The VC dimension of GNN described by Equations (13)-(15) is bounded by

$$\text{VCdim}(\Phi) \leq 2 \log B + \bar{p}(16 + 2 \log \bar{s}).$$

where  $\bar{p} = (2d + 1)(d(L - 1) + q + 1) - q$ ,  $\bar{s} = LNd + Nq + 1$  hold.

Thus, we can finally bound the VC dimension a GNN in the specific case when a logistic sigmoid is used as an activation function.

**Proposition 15.** The VC dimension of a GNN, when  $\sigma = \text{logsig}$ , is bounded by

$$\begin{aligned} \text{VCdim}(\text{GNN}) &\leq ((2d + 1)(d(L - 1) + q + 1) - q)^2(LNd + 1)^2 + \\ &\quad + 2((2d + 1)(d(L - 1) + q + 1) - q) \log(17) \\ &\quad + 2((2d + 1)(d(L - 1) + q + 1) - q) \log(20((2d + 1)(d(L - 1) + q + 1) - q)) \\ &\quad + ((2d + 1)(d(L - 1) + q + 1) - q)(16 + 2 \log(LNd + Nq + 1)) \end{aligned} \quad (16)$$

*Proof.* From Lemmas 7 and 13, we have

$$\begin{aligned} \text{VCdim}(\text{GNN}) &\leq 2 \log B + \bar{p}(16 + 2 \log \bar{s}) \\ &\leq 2 \log \left( 2^{\frac{\bar{\ell}(\bar{\ell}-1)}{2}+1} (\bar{\alpha} + 2\bar{\beta} - 1)^{\bar{p}-1} ((2\bar{p} - 1)(\bar{\alpha} + \bar{\beta}) - 2\bar{p} + 2)^{\bar{\ell}} \right) + \bar{p}(16 + 2 \log \bar{s}) \\ &= \bar{\ell}(\bar{\ell} - 1) + 2(\bar{p} - 1) \log(\bar{\alpha} + 2\bar{\beta} - 1) + 2\bar{\ell} \log((2\bar{p} - 1)(\bar{\alpha} + \bar{\beta}) - 2\bar{p} + 2) \\ &\quad + \bar{p}(16 + 2 \log \bar{s}) + 2 \end{aligned}$$

Let us assume that the activation function is the logistic sigmoid, whose format is  $(2, 1, 1)$ <sup>2</sup>. Then, it follows

$$\begin{aligned} \text{VCdim}(\text{GNN}) &\leq \bar{p}H(\bar{p}H - 1) + 2(\bar{p} - 1) \log(9) \\ &\quad + 2\bar{p}H \log(16\bar{p} - 7) \\ &\quad + \bar{p}(16 + 2 \log(\bar{s})) + 2 \\ &\leq \bar{p}^2 H^2 + 2\bar{p} \log(9) \\ &\quad + 2\bar{p}H \log(16\bar{p}) \\ &\quad + \bar{p}(16 + 2 \log(\bar{s})) \end{aligned}$$

---

<sup>2</sup>Notice  $\partial \text{logsig}(x) / \partial x = \text{logsig}(x)(1 - \text{logsig}(x))$ . Thus  $\text{logsig}$  is Pfaffian whose chain consists of the function itself,  $\beta_{\text{logsig}} = 1$  and  $\alpha_{\text{logsig}} = 2$ .

Then, by replacing  $\bar{p}$ ,  $H$  and  $\bar{s}$ , it follows

$$\begin{aligned} \text{VCdim}(\text{GNN}) &\leq ((2d+1)(d(L-1)+q+1)-q)^2(LNd+1)^2 \\ &\quad + 2((2d+1)(d(L-1)+q+1)-q)\log(9) \\ &\quad + 2((2d+1)(d(L-1)+q+1)-q)\log(16((2d+1)(d(L-1)+q+1)-q)) \\ &\quad + ((2d+1)(d(L-1)+q+1)-q)(16+2\log(LNd+Nq+1)), \end{aligned}$$

which is the thesis.  $\square$

On the base of the above theorem, we can derive the orders of growth of the VC dimension w.r.t. the dimension of the features, the number of the layers and the graph dimension, obtaining Theorem 4.

#### A.4 Proof of Theorem 5

The developed theory is easily adapted to the case where nodes can be grouped according to their colors so as defined by the Weisfeiler-Lehman algorithm. Since, a group of nodes with the same color are computationally equivalent, then the corresponding equations can be merged. Formally, for a given graph  $G$ , let  $C_1(G) = \sum_{t=1}^L C^t(G)$  be the number of colors generated by 1-WL, where  $C^t(G)$  is the number of colors at step  $t > 0$ . Moreover, let us assume that  $C^t(G)$  is bounded in the domain, namely there is  $C_1$  such that  $C_1(G) \leq C_1$  for all the graphs  $G$  in the domain. Similarly, let  $C_0(G)$  be the number of colors of the graph generated by 1-WL at the initial step and assume that there exists  $C_0$  such that  $C_0(G) \leq C_0$  for all the graphs of the domain.

Then  $s_c = C_1d + C_0q + 1$  can be used in place of  $\bar{s}$  in Lemma 14. Moreover, also the chains of the Pfaffian functions in merged equations can be merged and we have  $H$  can be replaced  $H_c = C_1d + 1$ . Finally, the length of the chains  $\ell$  of Lemma 14 is replaced by  $\bar{\ell}_c = \bar{p}H_c\ell_\sigma$ . With the above changes, the following proposition follows.

**Proposition 16.** Assume a subset  $\mathcal{S} \subseteq \mathcal{G}$  and consider a GNN using  $\text{logsig}$  as an activation function. The VC dimension of the GNN satisfies

$$\text{VCdim}(\text{GNN}) \leq \bar{p}^2(C_1d+1)^2 + \tag{17}$$

$$2\bar{p}\log(9) + 2\bar{p}(C_1d+1)\log(16\bar{p}-7) + \bar{p}(16+2\log((C_1d+C_0q+1))), \tag{18}$$



*Proof.* The proof follows by the same calculus in Proposition 15 and replacing  $H, \bar{s}, \ell$  with their corresponding values based on colors.

$$\begin{aligned}
\text{VCdim}(\text{GNN}) &\leq \bar{p}H_c(\bar{p}H_c - 1) + 2\bar{p}\log(9) \\
&\quad + 2\bar{p}H_c\log(16\bar{p} - 7) \\
&\quad + \bar{p}(16 + 2\log(\bar{s}_c)) + 2 \\
&\leq \bar{p}^2(C_1d + 1)^2 + 2\bar{p}\log(9) \\
&\quad + 2\bar{p}(C_1d + 1)\log(16\bar{p} - 7) \\
&\quad + \bar{p}(16 + 2\log((C_1d + C_0q + 1))), .
\end{aligned}$$

□

Notice that intuitively the presence of colors simplifies the graph. Actually, the bound of Equation 18 is almost identical to the one in 16, where the number of nodes of the input graph are decreased accordingly to colors.

## B Experiments on other datasets

In this Section we report the additional results on the experiment E1, regarding the evolution of the difference between the training and the test set, for GNNs with activation function  $f \in \{\arctan, \tanh\}$  over a dataset  $\mathcal{D} \in \{\text{PROTEINS}, \text{PTC\_MR}\}$ . Each figure shows the evolution of `diff` through the epochs, for certain values of `hd` keeping fixed  $l = 3$ , and for certain values of  $l$  keeping fixed `hd` = 32; for each Figure, the picture on the left shows how `diff` evolves as the hidden size increases, for certain epochs, while the picture on the right shows how `diff` evolves as the hidden size, or the number of layers, increases.

### B.1 Results for task E1: GNNs with activation function `arctan`

### B.2 Results for task E1: GNNs with activation function `tanh`

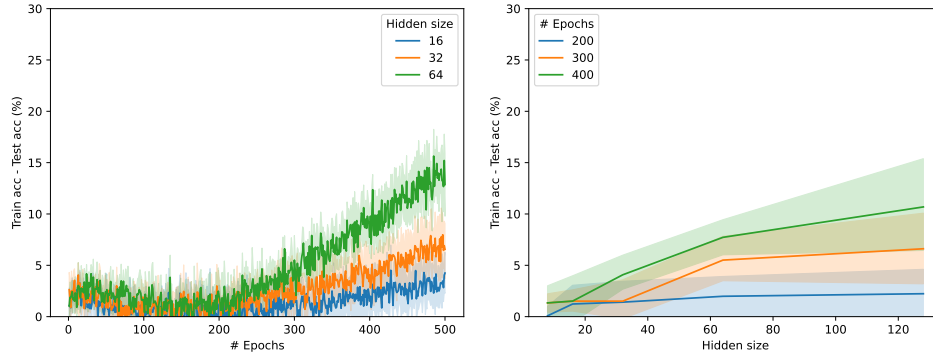


Figure 5: Results on the task **E1** for GNNs with activation function **tanh** over the dataset **PROTEINS**.

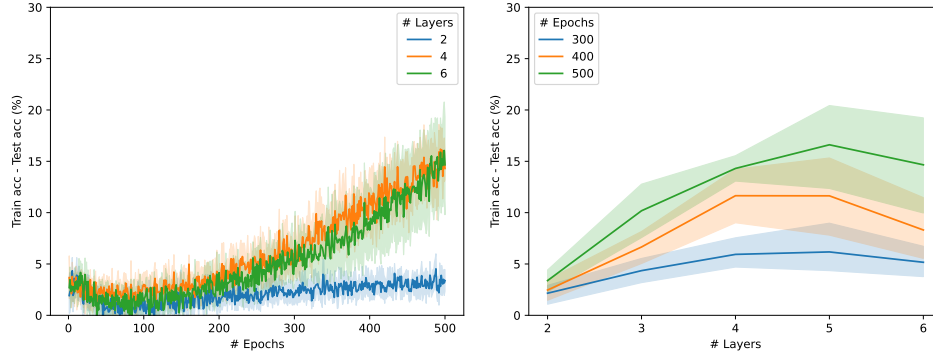


Figure 6: Results on the task **E1** for GNNs with activation function **atan** over the dataset **PROTEINS**.

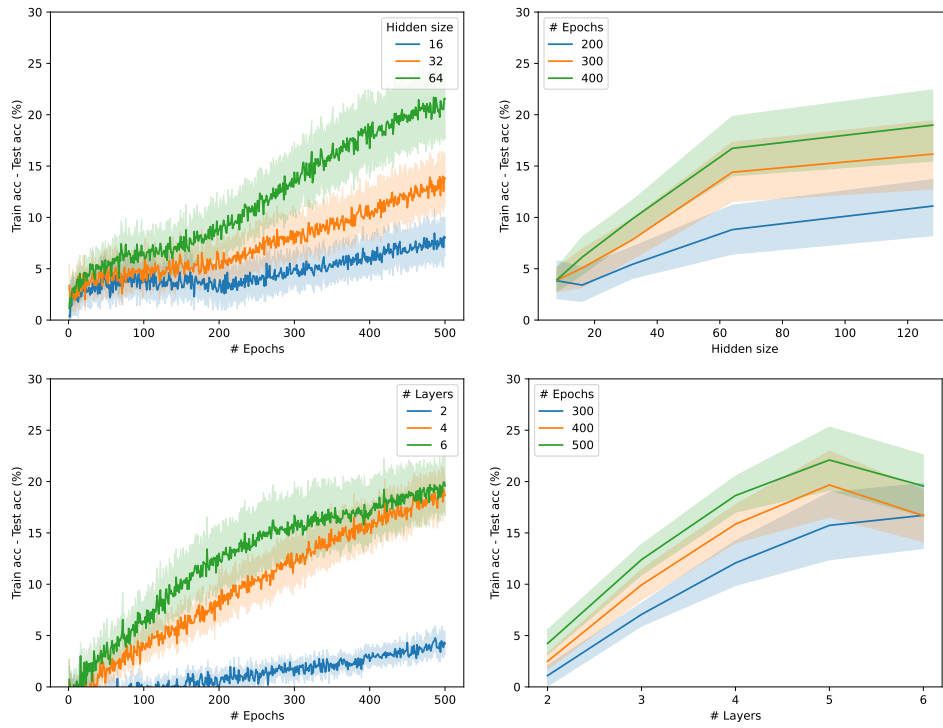


Figure 7: Results on the task **E1** for GNNs with activation function `atan` over the dataset `PTC_MR`.

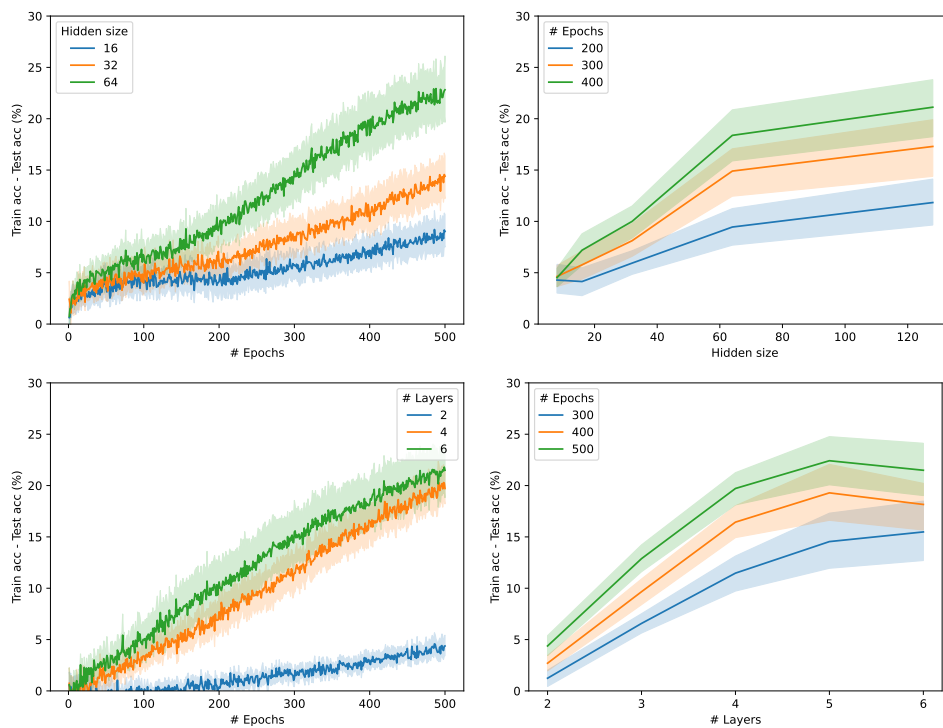


Figure 8: Results on the task **E1** for GNNs with activation function **tanh** over the dataset **PROTEINS**.

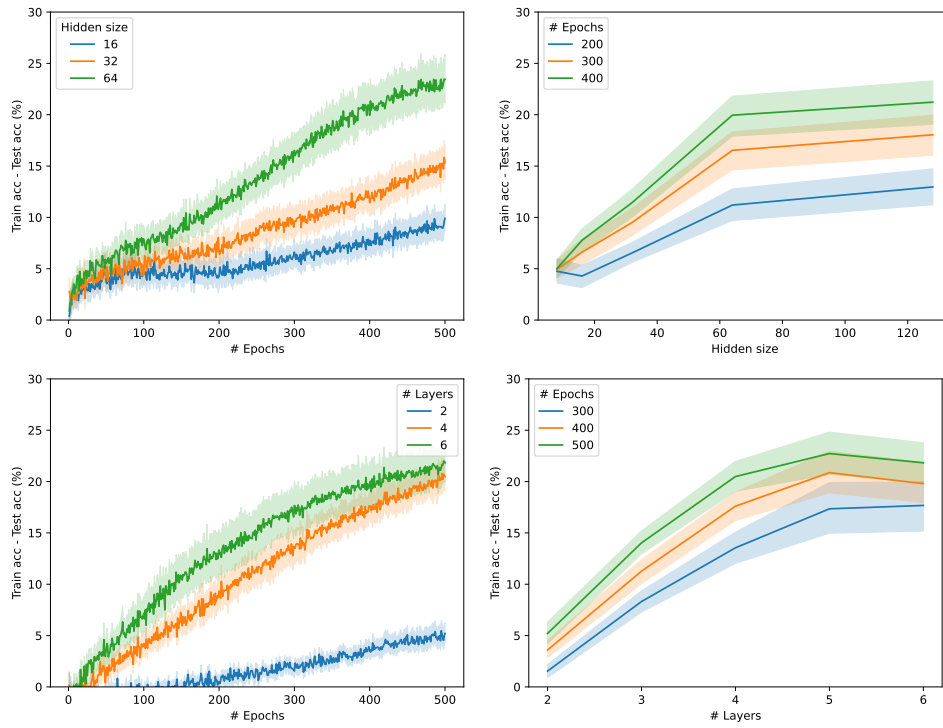


Figure 9: Results on the task **E1** for GNNs with activation function  $\tanh$  over the dataset PTC\_MR.